Phase Synchronization in Chaotic Systems

Krešimir Josić
Department of Mathematics and Statistics and Center for BioDynamics, Boston University, Boston, MA 02215

Douglas J. Mar
Department of Biomedical Engineering and Center for BioDynamics, Boston University, Boston, MA 02215
(June 27, 2000)

The geometric theory of phase locking between periodic oscillators is extended to phase coherent chaotic systems. This approach explains the qualitative features of phase locked chaotic systems and provides an analytical tool for quantitative predictions about the phase locked state in such systems. We apply the techniques to a simple chaotic system and find that both numerical simulations and data from electronic circuit experiments agree well with theoretical predictions.

05.45.Xt, 05.40.-a

Introduction Although phase locking between periodic systems has been studied at least since Huygens, the investigation of phase locked chaotic systems has a more recent history. Its occurrence was first noted in [1], and examined in more detail in [2]. It has been observed in electrically coupled neurons [3,4], spatially extended ecological systems [5], earthquake models [6], a plasma discharge tube [7], and its potential role in brain functions has been recognized [8].

Although much work has been done on detecting chaotic phase synchronization (CPS), a full understanding of the phenomenon and predictive methods are still lacking. Since periodic orbits form a skeleton of a strange chaotic attractor, it was argued in [9] that CPS can be described in terms of the phase locking properties of these periodic orbits. The phase dynamics of a driven chaotic system may also be modeled by a stochastically driven overdamped particle [10,11]. The detailed structure of attractors in the CPS regime was analyzed in [12]. These descriptions predict behavior that agrees well with that observed in systems exhibiting CPS, but offer no predictive methods for computing when and how CPS occurs.

In this Letter we extend the perturbative techniques used in the study of coupled periodic systems to analyze CPS in a driven chaotic system. Our approach reproduces some of the qualitative CPS behavior mentioned above. We apply these techniques to a periodically driven chaotic electronic circuit and show how it can be used to predict when and how CPS occurs in this system.

CPS in terms of perturbed isochrons Our approach follows that described in [13] for systems $\mathbf{X}' = \mathbf{F}(\mathbf{X})$ with an exponentially stable limit cycle ρ of period T. It is possible to find coordinates $(\phi, \mathbf{R})$ in a tubular neighborhood N of ρ so that the phase ϕ measures the distance along ρ, $\mathbf{R}$ measures the radial distance from ρ, and $\phi' = d\phi/dt = 1$. The solutions of $\phi = c$ are called *isochrons* and define codimension one manifolds that foliate N. An isochron consists of all points in N that approach a single point in ρ in forward time. If the system is driven by a small, periodic drive $\epsilon\mathbf{p}(t)$ with period T_d so that $\mathbf{X}' = \mathbf{F}(\mathbf{X}) + \epsilon\mathbf{p}(t)$, a direct calculation gives

$$\phi' = 1 + \epsilon\nabla_{\mathbf{X}}\phi \cdot \mathbf{p}(t) \stackrel{\text{def}}{=} 1 + \epsilon\Omega(\phi, t). \tag{1}$$

Since $\nabla_{\mathbf{X}}\phi$ points along the direction of the fastest increase of ϕ, it may be interpreted as the phase-dependent sensitivity. Hence $\epsilon\Omega(\phi, t)$ is the influence of the external drive on the phase. Defining the phase difference between drive and response as $\Psi = \phi - \frac{T}{T_d}t$ and letting $\epsilon\Delta = 1 - \frac{T}{T_d}$, we obtain

$$\Psi' = \epsilon[\Delta + \Omega(\frac{T}{T_d}t + \Psi, t)]. \tag{2}$$

Averaging over one period of the drive leads to

$$\Psi' = \epsilon[\Delta + \Gamma(\Psi)], \tag{3}$$

where $\Gamma(\Psi) = \frac{1}{T_d}\int_0^{T_d}\Omega(\frac{T}{T_d}t + \Psi, t)dt$.

If equation (3) has a stable fixed point Ψ_0, then the phase ϕ approaches the solution $\phi(t) = \Psi_0 + \frac{T}{T_d}t$, and the driven system approaches a periodic orbit $\mathcal{O}(\epsilon)$ close to ρ which is phase locked with the drive.

In what follows we assume that the system $\mathbf{X}' = \mathbf{F}(\mathbf{X})$ possesses a chaotic attractor A and that there exist coordinates $(\mathbf{R}, \phi)$ on A such that the equations of motion have the form

$$\mathbf{R}' = \mathbf{F}(\mathbf{R}, \phi) \tag{4}$$

$$\phi' = 1 + \delta(\mathbf{R}, \phi) \tag{5}$$

where $\phi(t + T) = \phi(t)$, $\delta(\mathbf{R}, \phi)$ is a small, residual term, and T corresponds to the approximate natural period of the attractor [14]. The residual term δ leads to phase diffusion, but if this term is small the phase ϕ increases nearly uniformly in time. Therefore systems for which the term δ is small may be called *phase coherent*. These definitions agree with those in [2].

It is reasonable to assume that the change of coordinates given by equations (4) and (5) can be extended to a neighborhood of A. Notice that the level surfaces of ϕ

no longer define isochrons in a strict sense, but consist of points that all approach a subset of approximately equal phase on A before diverging due to phase diffusion. Thus the coordinates $(\mathbf{R}, \phi)$ are not uniquely defined as in the periodic case, but are chosen so that the convergence to A is much faster than the phase diffusion due to δ.

If $\delta(\mathbf{R}, \phi)$ is small, we expect the phase in (5) to behave similarly to the phase in (1) when the chaotic system is periodically driven. More precisely, if the perturbed system has the form $\mathbf{X}' = \mathbf{F}(\mathbf{X}) + \epsilon\mathbf{p}(t)$, a straightforward application of the averaging theorem [15] yields

$$\Psi' = \epsilon[\Delta + \Gamma(\Psi)] + \delta(\mathbf{R}, \phi(\Psi, t)). \tag{6}$$

where Ψ, Δ and Γ are defined as above. Equation (6) is of form (3), with an additional small chaotic perturbation $\delta(\mathbf{R}, \phi(\Psi, t))$, the exact nature of which depends on the driven system. Assume that Ψ_0 is a stable fixed point of equation (3) and define the region

$$\mathcal{W} \stackrel{\text{def}}{=} \{\Psi : \min \delta < \epsilon[\Delta + \Gamma(\Psi)] < \max \delta\}. \tag{7}$$

For ϵ sufficiently large, $\mathcal{W}$ is a proper subset of $[0, T_d]$. If we let W be the component of $\mathcal{W}$ containing Ψ_0, then a simple Lyapunov function argument shows that W is a stable inflowing region. Thus, for ϵ sufficiently large, Ψ is trapped in the "wedge" W and the phase ϕ is phase locked to the drive with approximate phase difference Ψ_0.

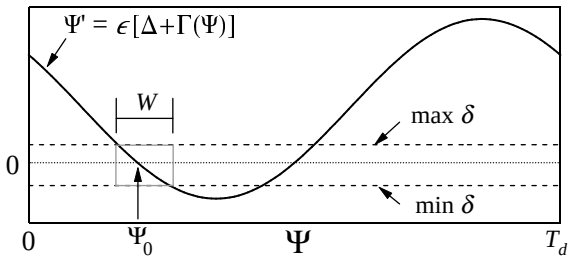

FIG. 1. Schematic representation of Eq. (6) for Ψ'. Once in the interval W, the relative phase cannot escape. The value of Ψ_0 estimates the phase difference between the drive and the system response, and the size of W estimates the variation in this difference.

For periodic systems the transition to phase locking occurs as follows: As ϵ increases, the graph (see Fig. (1)) of $\epsilon[\Delta + \Gamma(\Psi)]$ is dilated vertically. The unperturbed system (3) nears a saddle-node bifurcation and Ψ spends more time in the vicinity of the incipient bifurcation. At a critical value of ϵ, the driven system (3) undergoes a saddle-node bifurcation, giving birth to a stable fixed point Ψ_0. At this point the system enters the $1:1$ Arnold tongue and phase locks to the drive. The transition to CPS in the perturbed system (6) is similar, but more gradual. Even as the saddle-node bifurcation gives rise to a stable point Ψ_0 of (3), the residual term δ in (6) may cause the phase to slip out of a neighborhood of Ψ_0. As ϵ grows, these slips become rarer and disappear altogether with the creation of a trapping region for the phase. If $\max \delta$ and $\min \delta$ remain approximately constant as ϵ is increased, then the region W moves and becomes narrower, and so phase locking typically becomes tighter. This is illustrated in Fig. 2.

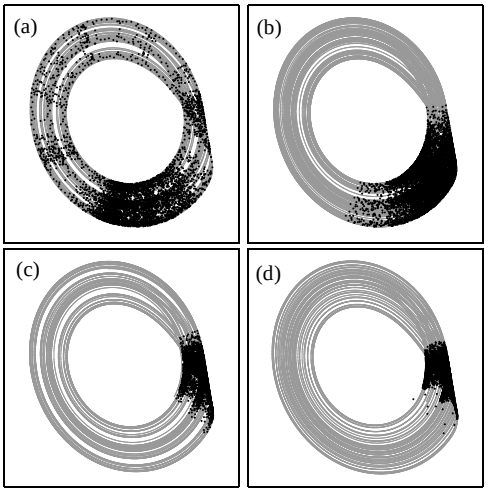

FIG. 2. Numerical simulations of system (8) for $\gamma = 0.10$, driven in y using $\epsilon \sin(\omega_d t)$ with $\omega_d = 0.711$. In (a)–(d), $\epsilon = 0.002,\ 0.005,\ 0.02,\ 0.05$ and the region plotted in each panel is given by $-4.3 \le x \le 4.3$ and $-5.8 \le y \le 5.1$. The dark points show the Poincaré section at zero drive phase. For $\epsilon = 0$ (data not shown), the points are distributed relatively evenly over the attractor. In (a), ϵ is small and the points become concentrated near $\Psi = -\pi/2$, but frequent phase slip events are still evident. As ϵ increases, these events become less frequent and eventually a phase locking region appears (b). For still larger ϵ, the region moves towards $\Psi = 0$ (c) and becomes narrower (d). For larger γ (data not shown), δ is larger and the trapping region is correspondingly broader. When the drive is applied to the x variable (data not shown), $\Psi \approx -\pi$ at the threshold of locking, and Ψ approaches $-\pi/2$ for large ϵ.

Remark 1 The existence of the region W is a sufficient, but not necessary condition for CPS. The attraction to an approximately phase locked state may become stronger than the phase diffusion even before the coupling is sufficiently strong for the region W to appear.

Remark 2 We note that $\delta(\mathbf{R}, \phi(\Psi, t))$ is a *deterministic* noise term. A more careful analysis of this term may lead to additional information about the phase locked state. For instance, in [16] this term is usually small, but occasionally it becomes large and leads to an intermittent loss of phase synchrony. Statistical information about these increases in δ yields direct information about the frequency of phase slips in such systems [17].

If $T_d > T$, then $\epsilon\Delta > 0$ and the graph of $\Gamma(\Psi)$ is shifted upwards. Then we expect δ to typically cause a forward slip in the phase ϕ. If $T_d < T$, the opposite is true.

In this argument, we implicitly assumed that $\nabla_{\mathbf{X}}\phi$ is approximately constant in a neighborhood of A for a fixed value of ϕ [18]. It was also assumed that the periodic driving has only a small effect on δ. Most importantly, ϵ must be small enough for the averaging theorem to hold, but sufficiently large for a phase trapping region to appear. These two opposing conditions on ϵ may not always be compatible and it is therefore necessary to treat phase-coherent attractors case by case. Fortunately, the perturbation results often hold for values of ϵ outside of those regions in which they can be justified rigorously. We therefore expect that the outlined approach will be applicable to a broad class of systems. A rigorous treatment of these issues is under current investigation.

Application to experiments To experimentally confirm the analysis above, we constructed a phase-coherent chaotic electronic circuit modeled by the following equations

$$\begin{aligned} x' &= -\alpha(x/20 + y/2 + z) \\ y' &= -\alpha(-x - \gamma y) \\ z' &= -\alpha[-15(x-3)\theta(x-3) + z], \end{aligned} \tag{8}$$

where $\theta(x)$ is the step-function and $\alpha = 10^4$ sets the experimental time scale. System (8) is a piecewise linear version of the Rössler system [19] and is the same as that used in previous studies of chaotic synchronization [20]. For experimental circuit details, see [21].

The phase space of (8) is divided into two regions, $R_1 = \{(x,y,z) \in \mathbb{R}^3 : x < 3\}$ and $R_2 = \mathbb{R}^3 - R_1$, in each of which the equations are linear. By changing coordinates so that the system is in normal form in R_1, the solutions of (8) in R_1 have the form

$$(w(t), z(t)) = e^{(\nu + i\omega)t} w(0) + e^{-t} z(0), \tag{9}$$

where $w(t) = x(t) + iy(t)$. In R_1 the solutions approach the xy plane, which is invariant. If $\gamma > 0.05$, then $\nu > 0$ and the origin is a spiral source in the xy plane. The parameter γ controls the instability of the origin since ν increases with increasing γ.

When an orbit enters R_2, it is lifted off the xy plane by the first term in the z' equation in (8). Shortly thereafter, the orbit is reinjected into R_1 closer to the z axis. This orbit quickly approaches the xy plane and, if $\nu > 0$, spirals outwards until it re-enters R_2 and the process repeats. In [22] it was shown that this behavior induces a Poincaré return map similar to the Hénon map, leading to chaotic behavior as in the Rössler system.

This system is particularly well-suited to test the approach outlined above, because in R_1 we can let

$$\phi = (\omega r)^{-1} \arctan(y/x) \tag{10}$$

where r is the average attractor radius, which depends on ν. It follows that in R_1 the sets $I_c = \{\phi : \phi = c\}$ form an invariant family, $\phi' = 1$, and $\nabla_{\mathbf{X}}\phi$ is constant on each I_c. These observations permit a straighforward calculation of $\Gamma(\Psi)$. Since all orbits eventually enter the region R_2, this description of the phase is incomplete. However, the size of the errors in this approximation depend directly on the size and frequency of the excursions into the region R_2. These in turn depend on ν, which can be directly controlled in experiments via the parameter γ. This allows us to adjust the magnitude of δ in (6).

Numerical and physical experiments were conducted by adding a driving term $\epsilon \sin(\omega_d t)$ to the equation for y' in (8). Using (10) and the derivation described in the previous section, in normal coordinates we obtain

$$\Gamma(\Psi) = 0.021 \cos(\omega\Psi) - 0.1666 \sin(\omega\Psi) \tag{11}$$

for $\gamma = 0.127$ and $r = 5.12$. Returning to the original coordinates of system (8), we see that if the frequency of the drive ω_d is larger than the intrinsic frequency of the circuit ω_0 [23], i.e. $T_d < T$ and $\epsilon\Delta < 0$, we expect that the circuit first locks to the drive with a phase difference $\Psi \approx -\pi/2$ and that Ψ moves towards 0 as ϵ is increased. Similarly, if $\omega_d < \omega_0$ we expect that initially $\Psi \approx \pi/2$, and Ψ moves towards 0 as ϵ is increased. As illustrated, the theoretical analysis above yields good qualitative (Figs. 2 and 3) and quantitative agreement with the experimental data in the location, size, and shape of the phase-locked region (Fig. 3).

Within the Arnold tongue, the circuit oscillates chaotically, but remains phase locked to the drive [24]. For large ϵ, the drive may be so strong that it imposes periodic dynamics upon the circuit. This occurs at the top of Fig. 3(b). We plot only the points for the region of CPS beneath this. In Fig. 3, the small discrepancies between the analytical and experimental results may be accounted for by our simplistic treatment of the phase jumps that occur whenever the system moves through R_2. It is known that relaxation oscillators are easier to synchronize than equivalent phase oscillators [25]. Together with Remark 1 this may account for the slight overestimate of the forcing strength ϵ necessary for CPS to occur.

Here we have used the system (8) as an illustrative example because ϕ and $\Gamma(\Psi)$ can be computed in a straightforward manner. The ideas we have employed carry over to any system that possesses a phase coherent attractor. In general, it may be necessary to employ numerical estimates to find optimal coordinates $(\mathbf{R}, \phi)$. Once such coordinates are obtained, the response of the system to any given periodic signal may be predicted from $\Gamma(\Psi)$.

CPS is of particular interest since it may be expected at coupling strengths ϵ that are considerably smaller than those necessary for complete synchronization between coupled chaotic systems. Because the phase corresponds to a nearly neutral direction within the attractor A, only a small driving force is required to control and entrain it. The dynamics in the radial directions can be *more*

unstable and therefore more difficult to control and synchronize. Chaotic phase coherent systems can exhibit a richness of behavior while their phase dynamics is still easy to control, a property with important implications for biological and other systems [4].

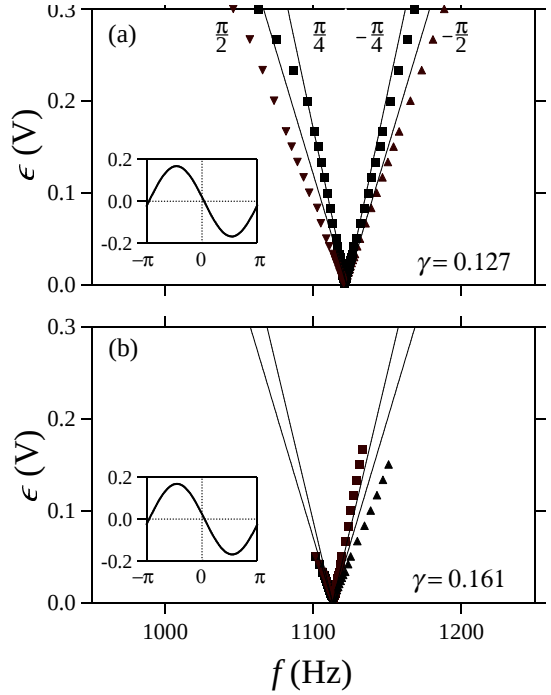

FIG. 3. CPS phase locking results from experiment (symbols) and theoretical analysis (lines) for system (8) for $\gamma = 0.127$ (a) and $\gamma = 0.161$ (b). The system is periodically driven in y with frequency and amplitude as shown on the axes. The average frequencies of the undriven system are 1122 Hz and 1113 Hz, corresponding to $\omega_0 = 0.705$ and 0.699, in (a) and (b). Triangles indicate when the system lies just at the threshold of slipping, while squares indicate parameters for which $|y| \approx |x|$ and $\Psi \approx \pm\pi/4$, as indicated at the top of (a). The wedge-shaped regions are analogous to Arnold tongues in the periodic case. The lines are calculated from $\Gamma(\Psi)$ and (3). Insets: $\Gamma(\Psi)$ vs Ψ, as obtained from (11) for (a). For (b) the coefficients of the terms in (11) are 0.025 and -0.1666.

In view of these arguments, we expect that our approach has applications beyond CPS. If there exists a change of coordinates in the neighborhood of a chaotic attractor such that in these coordinates certain directions are nearly neutral, we expect the system to be more malleable along these directions. Thus some coordinates may be easier to synchronize than others and partial synchrony may be achieved before full synchronization of the system occurs. We are currently investigating extensions of these ideas to bidirectionally coupled phase coherent chaotic systems.

We thank C.E. Wayne for useful discussions and M. K. S. Yeung for a critical reading of the manuscript.

[1] E. Stone, Phys. Lett. A **163**, 47 (1992).
[2] A. Pikovsky, M. Rosenblum, G. Osipov, and J. Kurths, Physica D **104**, 219 (1997).
[3] R. C. Elson, A. I. Selverston, R. Huerta, N. F. Rulkov, M. I. Rabinovich, and H. D. I. Abarbanel, Phys. Rev. Lett. **81**, 5692 (1998).
[4] V. Makarenko and R. Llinás, Proc. Natl. Acad. Sci. USA **95**, 15474 (1998).
[5] B. Blasius, A. Huppert, and L. Stone, Nature **399**, 354 (1999).
[6] M. de Sousa Vieira, private communication.
[7] E. Rosa, W. Pardo, C. M. Ticos, J. A. Walkenstein, and M. Monti, to appear in Int. J. of Bifurc. and Chaos.
[8] R. Fitzgerald, Phys. Today **17** (1999).
[9] A. Pikovsky, M. Zaks, M. Rosenblum, G. Osipov, and J. Kurths, Chaos **7**, 680 (1997).
[10] K. J. Lee, Y. Kwak, and T. K. Lim, Phys. Rev. Lett. **81**, 321 (1998).
[11] I. Kim, C. M. Kim, W. H. Kye, and Y. J. Park, submitted to Phys. Rev. Lett.
[12] E. Rosa, E. Ott, and M. H. Hess, Phys. Rev. Lett. **80**, 1642 (1998).
[13] Y. Kuramoto, *Chemical oscillations, waves, and turbulence* (Springer-Verlag, Berlin, 1984), pp. viii+156.
[14] M. Rosenblum, A. Pikovsky, and J. Kurths, Phys. Rev. Lett. **76**, 1804 (1996).
[15] J. Guckenheimer and P. Holmes, *Nonlinear oscillations, dynamical systems and bifurcations of vector fields* (Springer-Verlag, New York, 1983), pp. xvi+453.
[16] E. H. Park, M. A. Zaks, and J. Kurths, Phys. Rev. E **60**, 6627 (1999).
[17] V. Andrade,R. L. Davidchack, and Y.-C. Lai, Phys. Rev. E **61**, 3230 (2000).
[18] If $\nabla_{\mathbf{X}}\phi$ depends on R, a similar approach may be used if a physically significant invariant measure on A can be estimated. In this case the equivalent of (1) can be averaged with respect to that measure.
[19] O. E. Rössler, Phys. Lett. **57A**, 397 (1976).
[20] L. M. Pecora, T. L. Carroll, G. A. Johnson, D. J. Mar, and J. F. Heagy, Chaos **7**, 520 (1997).
[21] T. L. Carroll, Am. J. Phys. **63**, 377 (1995).
[22] C. T. Sparrow, J. Math. Anal. Appl. **83**, 275 (1981).
[23] Note that $\omega_0 > \omega$ (see (9)), due to the fast jumps in R_2.
[24] For each set of drive parameters in W, the circuit is monitored for more than 10^4 oscillation cycles to ensure that no slip events occur.
[25] D. Somers and N. Kopell, Biol. Cybern. **68**, 393 (1993).